

Provided for non-commercial research and education use.  
Not for reproduction, distribution or commercial use.



This article appeared in a journal published by Elsevier. The attached copy is furnished to the author for internal non-commercial research and education use, including for instruction at the authors institution and sharing with colleagues.

Other uses, including reproduction and distribution, or selling or licensing copies, or posting to personal, institutional or third party websites are prohibited.

In most cases authors are permitted to post their version of the article (e.g. in Word or Tex form) to their personal website or institutional repository. Authors requiring further information regarding Elsevier's archiving and manuscript policies are encouraged to visit:

<http://www.elsevier.com/copyright>



Contents lists available at ScienceDirect

Geoderma

journal homepage: [www.elsevier.com/locate/geoderma](http://www.elsevier.com/locate/geoderma)

## Extent and nature of organic coverage of soil mineral surfaces assessed by a gas sorption approach

Rota Wagai<sup>a,b,\*</sup>, Lawrence M. Mayer<sup>a</sup>, Kanehiro Kitayama<sup>b</sup>

<sup>a</sup> Ecology and Environmental Science Program School of Marine Science, Darling Marine Center, University of Maine, 193 Clarks Cove Road, Walpole, ME 04573, United States

<sup>b</sup> Center for Ecological Research, Kyoto University, 509-3 Hirano-cho, Ohtsu, Shiga 520-2113, Japan

### ARTICLE INFO

#### Article history:

Received 16 May 2008

Received in revised form 12 November 2008

Accepted 24 November 2008

Available online 3 January 2009

#### Keywords:

Specific surface area

Clay

Organic coating

Adsorption

Occlusion

Organo-mineral interaction

Aggregation

Altitude gradient

Soil organic matter

### ABSTRACT

Organic matter (OM) in soils often associates intimately with the surfaces of fine-grained minerals. We used two measures of OM–mineral associations, based on either the energetics of N<sub>2</sub> gas sorption (C-constant in BET equation) or changes in mineral specific surface area (SSA) upon removal of OM, that provide complementary information on organic coverage of mineral surfaces. Undisturbed surface mineral soils along an altitudinal transect in Borneo provided a gradient of OM levels (30 to 140 mg-OC g<sup>-1</sup> soil) with which to address modes of mineral surface coverage by OM, and were compared with a variety of soils throughout the USA. Increasing OM levels, either as OM content or as a ratio to SSA (i.e. loading), led to coverage of the mineral surfaces proportional to the OM content. In all surface horizon samples from Borneo and the USA, cross-plots of the two measures show that these surfaces were covered by OM having low SSA (presumably in globular forms) rather than thin coatings of adsorbed OM. The latter mode was found only in some podzolic B-horizon samples. At loadings of >3–4 mg-OC m<sup>-2</sup>, virtually all mineral surfaces in soils derived from aluminosilicate parent materials were covered by OM. Iron-rich soils on ultrabasic parent material did not achieve this full coverage. At loadings <2–3 mg-OC m<sup>-2</sup>, exposed surfaces of the soils were dominantly mineral even though 10–70% of total mineral surface was inaccessible to N<sub>2</sub> gas due most likely to organic occlusion of the mineral phases that have high SSA. These modes of OM-surface coverage may have important implications for aqueous–solid reactions in soil.

© 2008 Elsevier B.V. All rights reserved.

### 1. Introduction

Soil minerals provide extensive surfaces that strongly influence soil reactions occurring at aqueous–solid interfaces. Covering mineral surfaces with organic matter (OM) can inhibit sorption of ionic compounds (Lang and Kaupenjohann, 2003), enhance sorption of non-ionic compounds such as organic contaminants (Murphy et al., 1990; Wang et al., 2008), enhance or inhibit mineral dissolution (Welch and Vandevivere, 1994; Welch et al., 1999), and critically alter charge characteristics of soil surfaces (Chorover et al., 2004). In addition, the manner in which OM associates with mineral surfaces may influence OM stabilization in soils and sediments (e.g., Mayer, 1994; Kaiser and Guggenberger, 2003; Mayer et al., 2004). Yet little is known about the extent of organic coverage on soil mineral surfaces or the factors controlling it.

There are several approaches to assess soil mineral surface and its interactions with OM. Direct microscopy allows the characterization of physical features of OM–mineral associations in spatially-focused sections of soil. Using transmission electron microscopy, Chenu and Plante (2006) showed wide variations in the way OM covers or is encrusted by sub-micrometer mineral particles in <2 μm fractions from temperate soils. Elemental X-ray analysis of the SEM/TEM images showed spatial co-variations of OC with Fe, Al, and Si, suggesting important role of specific mineral components (e.g., phyllosilicate edges, iron oxides) in OM–mineral associations in submicron aggregates (Vrdoljak and Sposito, 2002). Even at maximum resolution, however, it is difficult to detect thin organic coatings on mineral surface (e.g., adsorption of low molecular-weight OM) by most current microscopic methods.

Another approach is based on the adsorption/desorption behavior of introduced gas molecules at surfaces, which allows characterization of much larger volume or mass of samples than microscopy. The gas sorption approach averages its results across all surfaces, and thus has a bias towards finer, clay-sized particles with much higher surface area per unit mass (specific surface area, SSA). Using the gas sorption approach with N<sub>2</sub> as surface probe, Mayer and Xing (2001) demonstrated variations in the extent and

\* Corresponding author. Current address: National Institute for Agro-Environmental Sciences, 3-1-3 Kan-nondai, Tsukuba, Ibaragi 305-8506, Japan. Tel.: +81 29 838 8327; fax: +81 29 838 8199.

E-mail address: [rota@affrc.go.jp](mailto:rota@affrc.go.jp) (R. Wagai).

nature of soil surfaces among acid soils and their different horizons. These approaches were extended by Kaiser and Guggenberger (2003) for a wider range of soils.

Significant increases in SSA of soil upon OM removal treatments indicate that organic covering of mineral surfaces generally reduces the exposed SSA of untreated soils (Feller et al., 1992; Pennell et al., 1995; Mayer and Xing, 2001; Kaiser and Guggenberger, 2003), because soil OM has low SSA ( $\sim 1 \text{ m}^2 \text{ g}^{-1}$ ) if measured by  $\text{N}_2$  sorption (Chiou 1990; Pennell et al., 1995; de Jonge and Mittelmeijer-Hazeleger, 1996; de Jonge et al., 2000; Mikutta et al., 2004; Kaiser and Guggenberger, 2007). For example, OM having low SSA likely covers or fills inter- or intra-particle pores associated with clay-sized mineral particles and their aggregates (Lang and Kaupenjohann, 2003; Mikutta et al., 2004; Kaiser and Guggenberger, 2007), reducing the  $\text{N}_2$ -accessible surface area of organo-mineral assemblages. All these organic associations with mineral components that lead to the reduction in SSA will hereafter be termed (organic) occlusion. The extent of the occlusion of mineral SSA can be parameterized as the proportion of mineral SSA that was liberated upon OM removal and is called, in this paper, the percentage of SSA occluded by OM (%  $\text{SSA}_{\text{occlusion}}$ ).

The enthalpy of  $\text{N}_2$  gas sorption, expressed as the C-constant in the Brunauer–Emmett–Teller (BET) equation (Brunauer et al., 1938), indicates if exposed surfaces are organic or inorganic, because  $\text{N}_2$  adsorbs onto less polar organic surfaces more weakly than onto more polar mineral surfaces (Mayer, 1999). The C-constant can be used to quantitatively determine the fractions of exposed surfaces that are organic or inorganic, by using a mixing equation between organic and inorganic endmembers (Mayer, 1999). This approach fails, however, as a quantitative measure of surface composition in some soils because of the presence of micropores (<2 nm diameter) that are often associated with iron and aluminum hydrous oxides (e.g., Mödl et al., 2007). Soil minerals with high microporosity have higher C-constant values compared to the soil minerals without them (Mayer and Xing, 2001) and the micropores are preferentially covered with OM compared to other parts of mineral surfaces in sorption experiments (Kaiser and Guggenberger, 2003; Mikutta et al., 2004; Filimonova et al., 2006). In addition, removal of OM by wet or dry oxidation treatments causes alteration and destruction of the micropores, reducing both SSA and C-constant (Mayer and Xing, 2001; Kaiser and Guggenberger, 2003; Filimonova et al., 2006). Nevertheless, a soil with full organic coverage of mineral surfaces can still be identified via a low C-constant of the untreated soil sample (i.e. no oxidation treatments).

These two measures of organic coatings of minerals provide similar but slightly different information. For example, consider

phyllosilicate clay particles that have high SSA largely due to nm-sized pores at the clay edges and intersections of particles. If a significant fraction of the pores are covered by OM but others exposed, then much SSA will be occluded. Nevertheless, the remaining, uncoated clay particles may still dominate the measured SSA and C-constant because their SSA is vastly greater than the SSA of organic matter coatings (as illustrated in Fig. 7 in Mayer and Xing, 2001). The manner in which these two parameters jointly respond to progressive loadings of OM should depend on the nature of the coatings and, conversely, the combination of these two parameters should provide unique insight into the nature of the coatings.

The aim of this study was to examine the patterns of organic coverage using these two parameters in the surface mineral soils under undisturbed forests along an altitudinal transect on Mt. Kinabalu (Borneo), where a previous study showed progressive increase in soil OM levels with altitude (Wagai et al., 2008). The C-constant and % $\text{SSA}_{\text{occlusion}}$  parameters were measured to assess the organic loadings necessary to cover mineral surfaces and to gain insight into OM–mineral associations in these soils. To corroborate the patterns found from this transect approach, we also examined a wider set of A-horizon soils as well as a smaller collection of B-horizon soils from different regions of the USA.

The term “mineral particle” is broadly defined in this paper to include mineral crystallites and less-crystalline phases, as well as their porous structures and aggregates.

## 2. Materials and methods

### 2.1. Study area

Study sites were located on the eastern and southern slopes of Mt. Kinabalu (4095 m, 6°05'N, 160°33' E) and are parts of long-term ecosystem study (Kitayama and Aiba, 2002). We selected six sites on the environmental matrix of three altitudes (at ca. 700, 1700, and 2700 m above sea level) and two parent materials (acidic meta-sedimentary and ultrabasic igneous rock). An additional site developed on Quaternary colluvium at 1860 m (Bukit Ular hill, see Kitayama et al., 2004) was selected for this study (Table 1). The study sites were more fully described in Kitayama and Aiba (2002) and Wagai et al. (2008). Briefly, the climate is humid tropical with weak influences of the Asiatic monsoon. Mean annual air temperature decreases from 24 °C at 700 m to 12 °C at 2700 m and mean annual rainfall is relatively constant (2300–2400 mm yr<sup>-1</sup>) with altitude (Kitayama, 1992). Soil water content increased from 27–35% to 136–

**Table 1**

Summary of site, soil chemical and mineralogical characteristics of Mt. Kinabalu study sites from previous studies

	Non-ultrabasic transect				Ultrabasic transect		
	700 m MS <sup>a</sup>	1700 m MS	1700 m QRT	2700 m MS	700 m UB	1700 m UB	2700 m UB
Altitude of each site (m)	650	1560	1860	2590	700	1860	2700
Mean annual air temperature (°C) <sup>b</sup>	24	19	17	13	23	17	12
Soil total OC (mg g <sup>-1</sup> ) <sup>c</sup>	29.8 (4.3)	49.1 (7.0)	80.6 (8.3)	142 (18)	30.3 (2.8)	62.1 (8.1)	83.0 (7.7)
C:N <sup>c</sup>	12 (0.4)	18 (1)	15 (0.3)	20 (1)	15 (1)	20 (1)	17 (0)
pH in deionized water <sup>c</sup>	3.9 (0.1)	4.1 (0.1)	3.9 (0.1)	3.9 (0.1)	4.8 (0.1)	5.4 (0.1)	4.9 (0.1)
Clay content (%) <sup>c</sup>	37.8	9.5	ND	14.8	45.6	16.6	24.3
Mineralogy of <2 μm fraction <sup>c</sup>	Kao, (Gib)	Kao, Ill, Qrt	ND	Kao, Ill	Hem, Got	Chl, Got, Tlc	Chl, Got, (Ill)
Dithionite-extr Fe (mg-FeOOH g <sup>-1</sup> ) <sup>d</sup>	33 (5.1)	13 (5.4)	9.8 <sup>e</sup> (0.3)	6.2 (2.3)	492 (10)	73 (23)	48 (2.6)

Standard errors (n=5) are in parentheses.

ND: not determined.

<sup>a</sup> Parent material abbreviation: MS = metasedimentary rock, QRT = Quaternary deposit, and UB = ultrabasic igneous rock.

<sup>b</sup> Based on the weather station at 2700 m and the lapse rate of 0.0055 °C per meter (Kitayama, 1992).

<sup>c</sup> From Wagai et al. (2008). Abbreviation in mineralogy: Kao = kaolinite, Gib = gibbsite, Ill = illite, Qrt = quartz, Hem = hematite, Got = goethite, Chl = chlorite, and Tlc = talc.

<sup>d</sup> Based on a modified dithionite extraction technique (Wagai and Mayer, 2007).

<sup>e</sup> From Kitayama et al. (2004) by conventional dithionite–citrate extraction (n=2) with superfloc sedimentation without high-speed centrifugation.

172% with altitude (Wagai et al., 2008) due to cooling and more frequent cloud cover at upper altitudes (Kitayama, 1992). Under the humid tropical regime, however, temperature appeared to exert stronger control on the forest structure, composition, productivity, and thus OM input rate than rainfall (Aiba and Kitayama, 1999; Kitayama and Aiba, 2002).

The metasedimentary parent material in the study area (Trusmadi formation) consists of Eocene argillite, slates, siltstones, and sandstones whereas the ultrabasic parent material consists mostly of peridotite, with various degrees of serpentinization, characterized by high concentrations of MgO, FeO, and heavy metals (Jacobson, 1970; Hutchison, 2005). Parent material at the Quaternary colluvium site is dominantly non-ultrabasic materials from upper altitudes (Jacobson, 1970). All seven sites were located on mid-slope positions (11–22°). Vegetation is classified as lowland rainforest dominated by Dipterocarpaceae at 700 m, lower montane rainforest at 1700 m, and upper montane rainforest at 2700 m (Aiba and Kitayama, 1999). Soils at lower altitudes are characterized by deeper solum, heavier texture, more weathered mineralogy, and higher pedogenic iron content (Table 1). According to Soil Taxonomy (Soil Survey Staff, 1999), soils were tentatively classified as Ultisol–Alfisol(Inceptisol)–Inceptisol from 700 to 2700 m on the metasedimentary series and Oxisol–Alfisol–Inceptisol on the ultrabasic series. The soil at the Quaternary colluvium site is also an Inceptisol which had little clay translocation in contrast to a nearby 1700-m metasedimentary site.

A companion study (Wagai et al., 2008) showed that total OC concentration in the surface 0–10 cm horizon increased with altitude on both parent material types (Table 1), which was mainly attributed to reduced decomposition rate under cooler (and wetter) climate at upper altitudes. The concentration of OC strongly bound to minerals (i.e.  $>1.6 \text{ g cm}^{-3}$  high-density fraction recovered after  $656 \text{ J mL}^{-1}$  ultrasound treatment) also increased from 22–26 to 50–67  $\text{mg C g}^{-1}$  soil from 700 to 2700 m in altitude (Wagai et al., 2008). While soil pH in water was always  $<5.5$ , the ultrabasic soils showed roughly 1-unit higher pH than metasedimentary soils at each altitude pair (Table 1).

## 2.2. Soil sampling and analyses of basic soil properties

We collected surface mineral horizon (0–10 cm) by a core sampler at five random locations at each site. Samples were 4-mm sieved, homogenized, and freeze-dried for gas sorption analyses. Details of soil sampling and handling as well as the methods used for basic soil properties (C, N, soil pH, clay mineralogy, and texture) were described in Wagai et al. (2008).

## 2.3. Sample pretreatment: pilot tests

### 2.3.1. Drying treatment

Water molecules in samples can cause large errors in gas sorption analysis, yet water-removal treatments may alter soil mineral phases (particularly less crystalline ones) and SSA. We thus first compared two drying techniques (helium gas flow at room temperature vs. heating at 150 °C under vacuum) using one sample from all seven sites. The four samples having high SSA ( $>10 \text{ m}^2 \text{ g}^{-1}$ ) showed minor changes in SSA between the two treatments (–6 to +17%), while the other three samples with low SSA ( $<10 \text{ m}^2 \text{ g}^{-1}$ ) had greater changes (–41 to +54%). We found no systematic change between the two treatments, and thus adopted the heating treatment due to better reproducibility.

### 2.3.2. OM-removal treatment

High SSA of soils can result from small particle sizes, surface roughness, nm-sized pores within or between particles, and/or low crystallinity. Soils with high SSA tend to be high in iron, aluminum,

and clay contents (e.g., Feller et al., 1992; Kaiser and Guggenberger, 2003) and store greater amounts of OM than low-SSA soils presumably due to intimate organo-mineral association (e.g., Mayer, 1994). Incomplete removal of OM prior to measurement likely results in an underestimation of the SSA of soil mineral component, as OM typically has much lower SSA than soil minerals (Pennell et al., 1995; de Jonge et al., 2000). Any technique of OM removal, however, alters less-crystalline mineral phases by various extents (Mikutta et al., 2005). Wet heating with hydrogen peroxide or dry heating reduces the SSA of hydrous metal oxides by sintering smaller pores and/or mineral transformations (Sequi and Aringhieri, 1977; Weidler and Stanjek, 1998; Mayer and Xing, 2001). Repeated sodium hypochlorite treatment (at room temperature, pH 8) reduced the alteration of less-crystalline hydrous metal oxides while 5–23% of initial OM remained after five cycles (Kaiser and Guggenberger, 2003) and up to 50% remained for subsurface horizons after three cycles (Mikutta et al., 2006).

To assess the tradeoff between incomplete OM removal and mineral alteration for our soil samples, we compared the difference in SSA by two techniques, (1) dry heating (muffling) at 350 °C overnight and (2) repeated hypochlorite oxidation (five cycles), using a representative surface sample from each site. Muffling showed more efficient OM removal and higher SSA, by up to 2-fold, compared to hypochlorite oxidation (Table 2). High stability of the OM sorbed on high-SSA sections of soil mineral (e.g., micropores) against hypochlorite oxidation (Mikutta et al., 2006; Kaiser and Guggenberger, 2007) likely explains the lower SSA after wet oxidation. Because the studied surface soils from Mt. Kinabalu contained relatively low amounts of poorly-crystalline Fe and Al oxides (Wagai and Mayer, 2007) and the SSA after muffling generally compared well with that after the  $\text{H}_2\text{O}_2$  treatment in sediments (Keil et al., 1997), we adopted the muffling technique to remove OM for this study. The muffling treatment, however, likely alters the SSA of iron oxides to an unknown extent. Dry heating at ca. 300 °C decreased the SSA of ferrihydrite by 40% but increased that of goethite by 120%, and 600 °C heating of the latter mineral dropped its SSA by 80% (Pritchard and Ormerod, 1976; Weidler and Stanjek, 1998). Thus we regard the SSA after our 350 °C muffling ( $\text{SSA}_{\text{muffled}}$ ) as a minimum value of the SSA of mineral components for the soils studied here.

## 2.4. Surface area and C-constant measurements

The gas sorption technique (Mayer, 1999) was used to measure SSA and assess the extent of organic coverage on mineral surfaces. Freeze- or air-dried samples were outgassed under vacuum at 150 °C. Gas sorption analysis was conducted using a Quantachrome

**Table 2**

Comparison of two OM removal pre-treatments with respect to the removal efficiency and specific surface area ( $n=1$  per site)

Altitude (m)	OC in bulk ( $\text{mg g}^{-1}$ )	Efficiency of OM removal by		Intact soil SSA ( $\text{m}^2 \text{ g}^{-1}$ )	SSA after NaOCl	SSA after muffling
		NaOCl (%)	Muffling (%)			
<i>Metasedimentary rock transect</i>						
700	27.6	80.1	97.6	26.4	27.9	32.0
1700	22.4	78.2	>98	7.3	6.6	10.9
2700	116	76.3	>98	3.7	6.2	12.4
<i>Ultrabasic rock transect</i>						
700	29.9	79.5	99.1	57.5	55.9	103
1700	44.0	64.4	>99	10.7	16.8	18.6
2700	93.9	64.8	>99	6.6	13.4	27.3

A-1 Autosorb (Quantachrome Corp., Boynton Beach, FL, USA) under a series of N<sub>2</sub> pressures. Surface area values were calculated using the multi-point BET approach (partial pressures of <0.3). After gas sorption analyses, samples were carefully transferred to beakers and muffled at 350 °C overnight. Upon cooling, the same outgassing and sorption analyses were performed on the muffled samples.

The C-constant is related to the enthalpy change upon sorption of N<sub>2</sub> gas molecule on surfaces, and was estimated from regression analysis of the data that rigorously obey the BET isotherm as described in Mayer (1999). The OM-removal treatments affect the C-constant value as well as SSA, particularly for metastable metal oxide phases (Mayer, 1999; Mayer and Xing, 2001; Kaiser and Guggenberger, 2003). We therefore only used the C-constant of untreated samples for the assessment of OM–mineral relationship. Because we suspected microporosity in some samples, we did not apply the quantitative methods of organic coverage based on enthalpies as done in Mayer (1999, 2005), and instead used only raw C-constant data for organic coverage assessment.

### 2.5. Derived parameters

The ratio of OC to mineral surface area (i.e. OC:SSA<sub>muffled</sub>, mg C m<sup>-2</sup>) is a useful measure to normalize changes in organic loadings of soil to grain size. This parameter, an averaged amount of OC loaded on mineral surfaces, is termed OC loading in this paper. Where data are available, we also calculated OC loading using the OC in the high-density fraction because major portions of OM in the low-density fraction are not in contact with mineral surfaces. The fraction of the total mineral surface area that was not accessible to N<sub>2</sub> gas in the untreated soils, due to organic occlusion of the mineral surfaces, was calculated following Mayer and Xing (2001):

$$\%SSA_{\text{occlusion}} = [(SSA_{\text{muffled}} - SSA_{\text{untreated}}) / SSA_{\text{muffled}}] \times 100$$

where SSA<sub>untreated</sub> and SSA<sub>muffled</sub> refer to the specific surface area of untreated and muffled soil, respectively.

OM content was also parameterized as the fraction of total solids' volume made up by OM (i.e. V<sub>OM</sub> / [V<sub>OM</sub> + V<sub>mineral</sub>]). This parameter gives a sense for the relative spatial scales of organic and mineral materials. For this calculation, we assumed an OM density of 1.4 g cm<sup>-3</sup> (Mayer et al., 2004) and OC content of 50% for the OM. At 700-m sites that have higher iron oxide contents, we used mineral densities of 2.8 and 4.6 g cm<sup>-3</sup> for metasedimentary and ultrabasic soils, respectively, based on pycnometry measurements (see Mayer et al., 2004). For the rest of the samples that are not highly weathered, the commonly-used mineral density of 2.6 g cm<sup>-3</sup> was used.

**Table 3**

Mineralogy, pedogenic iron oxide concentration, specific surface area and C-constant before and after muffling, organic occlusion of mineral surface, mean OC loading calculated with total OC and OC in high-density fraction

	Non-ultrabasic transect				Ultrabasic transect		
	700 m MS <sup>a</sup>	1700 m MS	1700 m QRT	2700 m MS	700 m UB	1700 m UB	2700 m UB
Untreated soil surface area (m <sup>2</sup> g <sup>-1</sup> )	25.5 <sup>b</sup> (2.4)	9.3 <sup>cd</sup> (2.4)	18.0 <sup>bc</sup> (2.1)	4.7 <sup>d</sup> (0.9)	59.6 <sup>a</sup> (3.0)	16.8 <sup>bc</sup> (1.4)	7.9 <sup>d</sup> (1.1)
Muffled surface area (m <sup>2</sup> g <sup>-1</sup> )	31.4 <sup>bc</sup> (2.4)	17.3 <sup>c</sup> (4.3)	43.4 <sup>b</sup> (2.1)	21.6 <sup>c</sup> (2.9)	96.7 <sup>a</sup> (6.7)	29.6 <sup>bc</sup> (2.8)	24.3 <sup>c</sup> (1.5)
Untreated soil C-constant	80 <sup>a</sup> (4)	51 <sup>b</sup> (13)	76 <sup>ab</sup> (7)	19 <sup>c</sup> (4)	87 <sup>a</sup> (2)	69 <sup>ab</sup> (4)	64 <sup>ab</sup> (4)
Muffled C-constant	110 <sup>b</sup> (2)	110 <sup>b</sup> (6)	99 <sup>ab</sup> (6)	150 <sup>a</sup> (13)	70 <sup>d</sup> (3)	66 <sup>d</sup> (2)	76 <sup>cd</sup> (3)
% mineral SSA occlusion by OM	19 <sup>e</sup> (2.6)	46 <sup>cd</sup> (2.8)	58.7 <sup>bc</sup> (3.8)	78 <sup>a</sup> (5.5)	38 <sup>d</sup> (2.5)	43 <sup>d</sup> (12.4)	68 <sup>ab</sup> (3.5)
OC <sub>Total</sub> :SSA <sub>muffled</sub> (mg-OC m <sup>-2</sup> )	1.0 <sup>cd</sup> (0.2)	3.8 <sup>b</sup> (1.2)	1.9 <sup>bcd</sup> (0.2)	6.9 <sup>a</sup> (0.9)	0.32 <sup>d</sup> (0.04)	2.1 <sup>bcd</sup> (0.1)	3.5 <sup>bc</sup> (0.4)
OC <sub>HF</sub> :SSA <sub>muffled</sub> (mg-OC m <sup>-2</sup> ) <sup>b</sup>	0.74 <sup>c</sup> (0.12)	2.2 <sup>ab</sup> (0.5)	ND	3.2 <sup>a</sup> (0.1)	0.27 <sup>c</sup> (0.03)	1.2 <sup>bc</sup> (<0.1)	2.1 <sup>ab</sup> (0.2)

Standard errors (n=5) in parentheses. Significant differences between sites are indicated by different letters (α=0.05).

ND: not determined.

<sup>a</sup>See Table 1 for abbreviation.

<sup>b</sup>The concentration of OC in high-density fraction (see text, also Wagai et al., 2008) normalized by the SSA of samples after muffling treatment.

### 2.6. Additional soil dataset

To test whether the pattern of organic coverage along the altitudinal transect in the tropical soils is applicable to wider range of soils with various OM loadings, we assembled thirty seven soil samples from various parts of the USA. General and surface-related characteristics are shown in Appendix A. Surface soil samples include 1 Histosol, 2 Entisols, 8 acid-leached soils (Inceptisols, Spodosols), 6 moderately-developed soils (Alfisols, Mollisols), and 4 weathered soils (Ultisols and an Oxisol). We also included sixteen B-horizon samples of the acid-leached soils. These samples were all 2-mm sieved and freeze-dried or air-dried. The acid-leached soils are from Mayer and Xing (2001), and most others are archived samples from Mayer et al. (2004) and Wagai and Mayer (2007), except for two samples. Those are an Alfisol from Indiana (0–23 cm) and an Ultisol from Maryland (0–13 cm), obtained from a soil archive (USDA, Soil Survey Center, Nebraska). Most surface horizon samples are cultivated (i.e. from Ap horizon, see Appendix A).

### 2.7. Data analysis

To compare the means of measured parameters among the seven sites in Mt. Kinabalu, the Tukey–Kramer HSD test was performed as an ad hoc test. All references to statistical significance were based on a 5% probability level. Pearson product-moment correlation was used to find correlation between the C-constant of untreated samples and OC:SSA<sub>muffled</sub> ratios as well as between %SSA<sub>occlusion</sub> and volumetric OM content. All statistical analyses were conducted using JMP version 6.0.3 (SAS Institute Inc.).

## 3. Results

### 3.1. Soil surface area and the ratio of OC:SSA

Variation in specific surface areas of soils before OM removal (i.e. SSA<sub>untreated</sub>) was strongly controlled by both altitude and parent material type. SSA<sub>untreated</sub> was significantly higher at the 700-m site than at upper altitudes on both parent materials (Table 3), consistent with more weathered mineralogy, heavier texture, and higher pedogenic iron content compared to upper altitude sites (Table 1). These pedological changes along the altitudinal gradient are generally attributable to climate, specifically faster chemical weathering under warmer climate. The relatively high SSA<sub>untreated</sub> from the soils at the 1700-m Quaternary colluvium site is an exception to the altitudinal trend, which presumably reflects different mineralogy of the site. At each altitude pair, the ultrabasic soil had higher SSA<sub>untreated</sub> than the metasedimentary soil (Table 3), as did the abundance of iron.

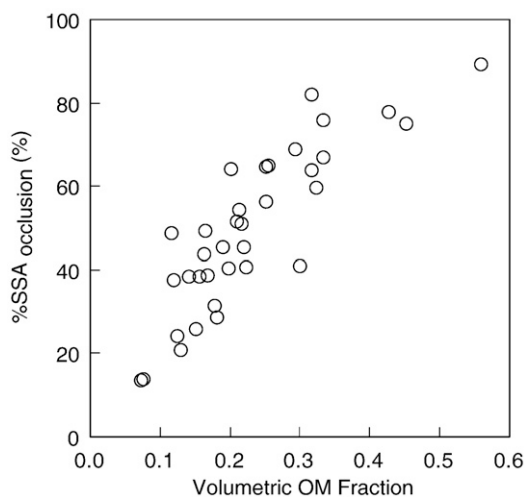


**Fig. 1.** The proportion of the surface area liberated by OM removal (%SSA<sub>occlusion</sub>) versus the volumetric fraction of OM (see Materials and methods for calculation). Among all the Kinabalu samples, significant positive correlation ( $r^2=0.72$ ,  $p<0.0001$ ) was found.

Specific surface area of soils after OM removal (i.e. SSA<sub>muffled</sub>) was always higher than that before OM removal and showed similar cross-site patterns to SSA<sub>untreated</sub> (Table 3). With increasing altitude, the OC:SSA<sub>muffled</sub> ratio (OC loading) increased from 0.3–1.0 to 3.5–6.9 mg-OC m<sup>-2</sup> and was higher in metasedimentary soils than in ultrabasic soils (Table 3).

### 3.2. C-constant and SSA reduction by OM

With increasing altitude and corresponding increases in total soil OC and OC loading (Tables 1, 3), the C-constant of untreated samples progressively decreased from 80 to 19 along the metasedimentary transect and from 87 to 64 along the ultrabasic transect (Table 3). The 1700-m Quaternary colluvium site was again the exception to this trend. The C-constant showed no systematic trends between the two parent materials. Across all sites, the untreated sample C-constant was inversely correlated to the OC:SSA<sub>muffled</sub> ratio ( $r^2=0.83$ ,  $p<0.001$ ). Similar inverse correlation ( $r^2=0.81$ ,  $p<0.001$ ) was found when the OC:SSA<sub>muffled</sub> ratio was calculated using the OC concentration in high-density fraction ( $>1.6$  g cm<sup>-3</sup>).

Upon OM removal by muffling, C-constants increased to 100–150 for the metasedimentary soils. For the ultrabasic soils, in contrast, muffling caused a drop in C-constant below the level of its unmuffled samples at lower altitudes (Table 3). This reduction likely resulted from transformation of metastable iron oxides in which high-energy micropores were reduced (Weidler and Stanjek, 1998; Mayer and Xing, 2001; Kaiser and Guggenberger, 2003). However, some iron oxides can have relatively low C-constants – e.g. 74 and 80 for hematite and 2-line ferrihydrite, respectively (Kaiser and Guggenberger, 2003). With the increase in OC concentration and OC:SSA<sub>muffled</sub> ratio proceeding up the altitudinal gradient, %SSA<sub>occlusion</sub> progressively increased from 19 to 78% along the metasedimentary transect and 38 to 68% along the ultrabasic transect (Table 3).

## 4. Discussion

### 4.1. Kinabalu surface soils along the altitudinal transect

We can assess the nature of the untreated soil surfaces that are exposed to N<sub>2</sub> gas molecules from their C-constants, because mineral surfaces generally have higher values (70–120) than organic

surfaces (20–40) (Mayer, 1999). The C-constants of muffled samples (Table 3) were within the range reported for naked surfaces of various mineral types (Mayer, 1999; Kaiser and Guggenberger, 2003). Low C-constants (<40) of untreated samples, that imply that most or all exposed surfaces were organic, were found only for the 2700-m metasedimentary soils where total soil OC concentration and OC:SSA<sub>muffled</sub> ratio were the highest across the sites (Table 3). All other Kinabalu soils had higher C-constants, indicating that uncoated mineral surfaces were significant or dominant contributors to total SSA.

The volume-based OM content was positively correlated with the %SSA<sub>occlusion</sub> parameter among the Kinabalu surface soils (Fig. 1). This correlation implies that mineral surfaces are occluded in direct proportion to the accretion of OM (which has low SSA) that surrounds high-SSA mineral particles. The surface area of minerals is generally held within micropores or mesopores that are formed by aggregation of primary grains such as sub-micrometer phyllosilicates or metal oxides (Mayer et al., 2004 and references therein), so that occlusion of aggregates can shield high-SSA internal pores with a low-SSA external sheath (Mayer and Xing, 2001; Kaiser and Guggenberger, 2003; Mikutta et al., 2004; Kaiser and Guggenberger, 2007; Mödl et al., 2007). The roughly linear relationship found here suggests that the probability of the organic occlusion of mineral surfaces may be directly proportional to the volume fraction of OM and is consistent with strong association between the OM and mineral grains as indicated by density separations (Wagai et al., 2008). Occlusion of submicron clay particles by OM has been directly observed by TEM in <2 μm fractions of some surface soils (Chenu and Plante, 2006).

These two ways of parameterizing surface coverage of minerals by OM (i.e. C-constant of untreated samples and %SSA<sub>occlusion</sub>) can be combined to provide additional insight in OM–mineral associations at μm to nm scales. Consider two simple cases for OM–mineral association. In the first, mineral surfaces are coated with a thin layer of organic matter which does not change the SSA measured prior to muffling (Fig. 2, A lines). With an increase in OM concentration, the C-constant decreases with only minor increase in %SSA<sub>occlusion</sub> in this

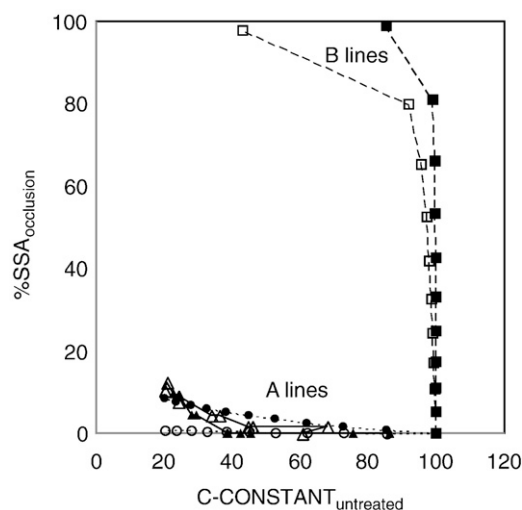


**Fig. 2.** Two end-member models of OM association with mineral surface as expressed on C-constant vs. %SSA<sub>occlusion</sub> plot. A lines (paint model) represent model trajectory of molecular-level adsorption of low molecular-weight organic compounds (○, ●). Additional lines are based on adsorption experiments (▲ lauric acid, △ stearic acid) on alumina (Mayer, 1999) B lines (occlusion model) represent model trajectory of organic occlusion of mineral surface as a function of volumetric OM fraction (■, □). Mineral grains with SSA of 10 m<sup>2</sup> g<sup>-1</sup> (open symbol) and 100 m<sup>2</sup> g<sup>-1</sup> (filled ones) were considered in the models. See Appendix B for assumptions and calculations.

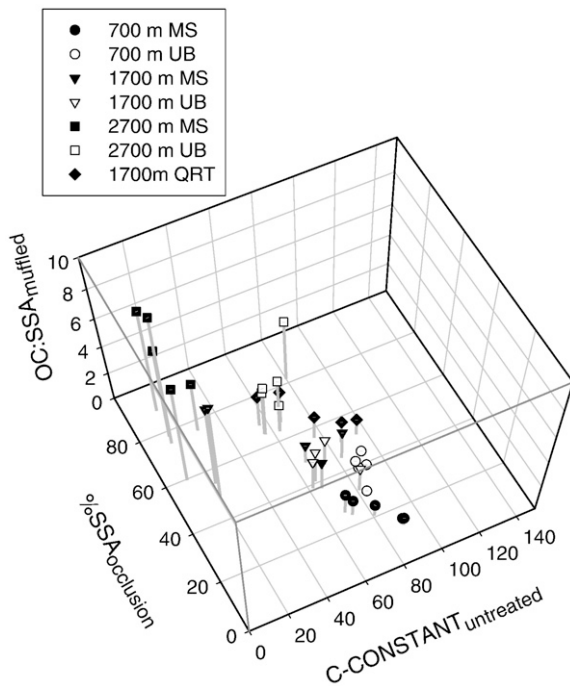


Fig. 3. Relationships among the untreated C-constant, %SSA<sub>occlusion</sub>, and OC:SSA<sub>muffled</sub> ratio for surface mineral soils from the seven sites in Mt. Kinabalu.

“paint” model trajectory. Adsorption of fatty acids on pure alumina showed this type of trajectory (unpublished data from experiments described in Mayer, 1999, Fig. 2, triangles). In the second case, minerals with a high SSA are occluded in a fashion linearly proportional to OM volume. In this “occlusion” model (Fig. 2, B lines), %SSA<sub>occlusion</sub> was calculated by assuming that the added OM occludes a volume of space containing mineral grains with a probability equivalent to the volume fraction of OM, replacing mineral surface area with the OM surface area. OM was assumed to have SSA of 1 m<sup>2</sup> g<sup>-1</sup> (Chiou 1990; Pennell et al., 1995; de Jonge and Mittelmeijer-Hazeleger, 1996; de Jonge et al., 2000; Mikutta et al., 2004; Kaiser and Guggenberger, 2007) and density 1.4 g cm<sup>-3</sup> (Mayer et al., 2004). The C-constants were derived from calculated organic coverage values using formulae of Mayer (1999, 2005). Calculation and assumption details are described in Appendix B. These two lines provide end-member trajectories that might accompany a series of samples varying in their organic matter loading.

We then plotted the field soil samples from Mt. Kinabalu on the same C-constant vs. %SSA<sub>occlusion</sub> plot, along with a third axis, OC:SSA<sub>muffled</sub> ratio, to illustrate how these surface-coverage parameters change with this measure of OM loading (Fig. 3). Sample data points generally fell closer to the occlusion model line, especially for the ultrabasic series. With the increase in OM loading that we found with increasing altitude, mineral soil surface appears to be covered via incorporation of fine-grained minerals into accumulating OM, in proportion to the fractional volume of OM as suggested in Fig. 1, rather than via molecular-level adsorption that efficiently coats all mineral surfaces. For example, in soils with high OM inputs, fine-grained minerals might be progressively occluded into biological secretions, or OM might fill high-SSA pores (e.g., small mesopores) within fine-grained aggregates (McCarthy et al., 2008).

A combination of low C-constant (e.g., <40) and high %SSA<sub>occlusion</sub> (>75%) would give strong indication that most mineral surfaces are fully occluded with low-SSA organic matter. Four of the five

metasedimentary soils from the 2700-m altitude showed this full coverage (Fig. 3). These samples had OC:SSA<sub>muffled</sub> ratios of 3.7–9.4 mg-OC m<sup>-2</sup>, the highest OM loadings we found among the whole Kinabalu soils. If we use only the OC in the high-density fraction (HF), these samples had OC<sub>HF</sub>:SSA<sub>muffled</sub> ratios of 3.0–3.2 mg-OC m<sup>-2</sup>. While it is possible to achieve full surface coverage at lower (~1) OC:SSA ratios via adsorption of low molecular-weight OM in the laboratory (unpublished experiments – Mayer, 1999), an OC:SSA<sub>muffled</sub> ratio of roughly 3–4 mg-OC m<sup>-2</sup> appeared necessary to achieve the full surface coverage in the natural environment on Mt. Kinabalu. Note that this level of OM loading is higher than the level required to saturate sorption sites on mineral surfaces in most laboratory experiments. When maximum sorption of naturally-occurring dissolved OM is reached at common soil pH values, OM loadings are no more than 2.3–3.4 mg-OC m<sup>-2</sup> for goethite and typically much lower for other minerals including phyllosilicate clays (Tipping, 1981; Benke et al., 1999; Chorover and Amistadi, 2001; Kaiser and Guggenberger, 2003; Mödl et al., 2007). While laboratory sorption doesn't often achieve full organic coverage (Kaiser and Guggenberger, 2003; Lang and Kaupenjohann, 2003; Mödl et al., 2007), OM association with goethite around maximum sorptive capacity (1.9 mg-OC m<sup>-2</sup> in this case) led to bulky OM accumulations presumably via hydrophobic interactions embedding some of the goethite particles (Kaiser and Guggenberger, 2007). None of the Kinabalu samples fell clearly into the zone of the “paint” model (i.e. low C-constant and low %SSA<sub>occlusion</sub>).

No ultrabasic soil samples exhibited full organic coverage, as indicated by relatively high C-constants, which may be related to lower OC:SSA<sub>muffled</sub> ratios or higher abundance of iron oxides compared to the metasedimentary soils (Tables 1, 3). Iron oxides can exhibit higher C-constants than phyllosilicates or alumina due to the abundance of micropores (Mayer and Xing, 2001; Kaiser and Guggenberger, 2003), which might make it more difficult to achieve

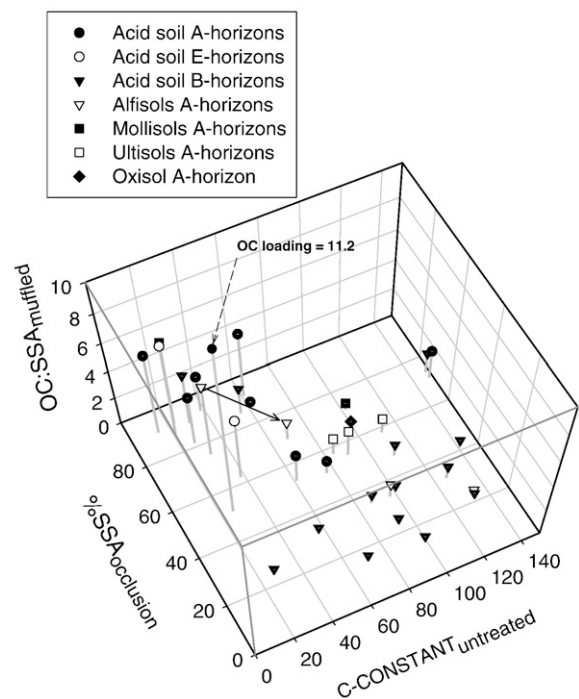


Fig. 4. Relationships among the untreated C-constant, %SSA<sub>occlusion</sub>, and OC:SSA<sub>muffled</sub> ratio for a variety of soils from the USA. Sample information is in Appendix A.

a low average C-constant. In addition, iron can dissolve and re-precipitate with changes in redox condition (Schwertmann, 1988); if this process occurs at the scales of occluded minerals then perhaps uncoated surface area is regenerated in response to reduced (lower Eh) microzones within OM occlusions. In this manner, uncoated iron-oxide surface area might be continually regenerated upon occlusion by OM at upper-altitude ultrabasic soils where OC and moisture contents are high. In Hawaiian volcanic soils on the lava age of 20–400 kilo years, iron and aluminum hydroxides rather than OM, appeared to dominate surface charge characteristics (Chorover et al., 2004).

#### 4.2. OM–mineral association in wider range of soils

We also examined a variety of A-horizon samples and a smaller collection of E- and B-horizon samples from different parts of the USA (Appendix A). The A- and E-horizon samples showed similar proximity to the occlusion trajectory as the Kinabalu surface soils (Fig. 4). At least five A-horizons, one E-horizon, and one B-horizon sample had both low C-constant (roughly <40) and high %SSA<sub>occlusion</sub> (roughly >75%), implying full organic coverage of mineral surfaces. These samples had comparable OC:SSA<sub>muffled</sub> ratios (2.7–6.7 mg-OC m<sup>-2</sup>) as the fully-covered Kinabalu soils. The uncultivated Albia Alfisol A-horizon is one of the samples with full organic coverage. The cultivated A-horizon sample from the same soil series (see arrow in Fig. 4) had significantly higher C-constant, lower %SSA<sub>occlusion</sub> and lower OC:SSA<sub>muffled</sub> ratio, in line with the overall trajectory of Kinabalu samples. Our result may be in accord with the TEM observation of an Inceptisol by Chenu and Plante (2006) who showed that OM reduction by cultivation led to a decrease in the abundance of (organo-clay) microaggregates and an increase of mineral particles in the <2 μm fraction.

In contrast to surface soils, we found that two of the B-horizon samples (Bw horizons of Inceptisols) had a combination of low C-constant and low %SSA<sub>occlusion</sub>, implying the “paint” type of OM–mineral association. It seems therefore possible to achieve the “paint” type association not only in the laboratory (Mayer, 1999 as discussed above) but also in natural soil environments. This “paint” type of association may result from molecular-level adsorption of low-molecular weight organic compounds onto highly adsorptive oxide phases, with little reduction of surface area. The subsurface horizons (Inceptisols and Spodosols from north-eastern USA) had high variation in C-constants despite low variation in %SSA<sub>occlusion</sub>. The variable C-constants are likely due to the less-crystalline iron and aluminum oxides with different degrees of microporosity (Mayer and Xing, 2001).

At OC:SSA<sub>muffled</sub> <3–4 mg-OC m<sup>-2</sup>, most of the surface soil samples from both Mt. Kinabalu and other regions were characterized by high C-constant values (roughly >60) suggesting abundant, naked mineral surfaces, despite a wide range in organic occlusion of mineral surfaces. For the sample group of lowest OC:SSA<sub>muffled</sub> ratios (≤1.0 mg-OC m<sup>-2</sup>, n=17), appreciable fractions of total mineral surfaces were still occluded by OM (%SSA<sub>occlusion</sub> range: 13–51%) while the high C-constants (72–95) indicate that exposed surface is dominantly uncoated mineral. Similarly, organo-mineral materials in near-shore sediments were largely characterized by high C-constants at low OC:SSA ratios (Bock and Mayer, 1999). These results suggest that, even at relatively low OC:SSA<sub>muffled</sub> ratio and low soil OM concentrations such as cultivated soils and weathered tropical soils, OM seems to be present as discrete patches (rather than thin, extensive coatings on mineral surfaces) with some of the patches occluding high-SSA mineral particles (e.g., sub-micrometer phyllosilicates and metal oxides) and reactive mineral topologies such as micropores (Mayer and Xing, 2001; Kaiser and Guggenberger, 2007). This

view of OM–mineral associations is in agreement with the conclusion based on a different gas sorption approach (Ravikovich et al., 2005) and appears consistent with (and complementary to) the results from electron microscopy, *in-situ* spectromicroscopy, and X-ray photoelectron spectroscopy (Myneni et al., 1999; Arnarson and Keil, 2001; Pichevin et al., 2004; Chenu and Plante, 2006).

#### 4.3. Implications for surface reactivity

This study has focused on measurement of mineral surfaces, and found that many surfaces are coated with OM. The coated surfaces, which may be only certain faces of mineral grains, will be protected to some extent from equilibration with the aqueous phase. Because surface area measurements are biased toward fine-grained minerals, our results will apply most strongly to the clay fractions. In soil systems with high organic loadings (e.g., >3–4 mg-OC m<sup>-2</sup>), virtually all fine-grained minerals should be protected. Conversely, in soils with <1 mg-OC m<sup>-2</sup>, there will be little of this type of protection. Thus factors controlling the organic matter loading – e.g. accumulation vs. decay – play an important role in mineral–water equilibration reactions via this influence on coatings (e.g., Chorover et al., 2004). Obviously there are other ways in which the OM cycle will also affect mineral–water reactions, such as generation of complexing acids, but this armoring impact of organic coatings should receive more attention than it has up to now.

### 5. Summary

The approach by Mayer (1999) to estimate the fractional organic coverage of material surfaces based on the difference in the C-constant before and after OM removal had limited applicability to soils with less-crystalline metal oxides and more microporosity, such as the ultrabasic soils from the Kinabalu sites and podzolic subsurface horizons, as previous studies pointed out (Mayer and Xing, 2001; Kaiser and Guggenberger, 2003). The C-constants of samples without OM oxidation treatment, nevertheless, allowed the detection of full organic coverage of mineral surfaces in soil. By comparing C-constants to the extent of mineral surface occlusion by OM (%SSA<sub>occlusion</sub>), it is possible to differentiate between occlusion and “painting” modes of OM association with mineral surfaces. At OC:SSA<sub>muffled</sub> ratios of >3–4 mg-OC m<sup>-2</sup>, both parameters indicate that most surfaces are fully covered with OM. Except for a few subsurface horizons dominated by “painted” surfaces, samples with OC:SSA<sub>muffled</sub> ratios <2–3 mg-OC m<sup>-2</sup> were characterized by the dominance of naked mineral surfaces despite appreciable extents of organic occlusion of other mineral surfaces (%SSA<sub>occlusion</sub> of 10–70%). A similar trajectory, from low %SSA<sub>occlusion</sub> and high C-constant towards the zone of full organic coverage for both Kinabalu (Fig. 3) and other soil samples examined here (Fig. 4), implies similar progression in OM–mineral association modes in response to increasing OC:SSA<sub>muffled</sub> ratio or OM concentration (expressed gravimetrically or volumetrically).

### Acknowledgement

This study was supported by NASA Earth System Science Fellowship Program (Grant NGT5), the American Chemical Society (Petroleum Research Fund), the U.S. Dept. of Agriculture, and Japanese MESSC (no. 18255003). Special thanks to the Sabah Park, Malaysia for generous field and laboratory support, and L. Schick for technical assistance throughout the project. We also thank K. Kaiser for valuable discussions, T. Reinsch (National Soil Survey Center, USDA) for sharing soils, and two anonymous reviewers for helpful comments. Contribution #409 of the Darling Marine Center.

Appendix A. General and surface-related characteristics of non-Kinabalu soil samples (from the USA) used for Fig. 4

Soil grouping	Location (state)	Soil series	Soil class (suborder)	Horizon and depth	Untreated soil					DC extraction		Clay content %	
					OC mg g <sup>-1</sup>	N mg g <sup>-1</sup>	SSA m <sup>2</sup> g <sup>-1</sup>	BET-C	SSA <sub>occlusion</sub> %	OC:SSA <sub>muffled</sub> mg-OC m <sup>-2</sup>	Fe %		Al %
Entisol/Histosol	MA	Swansea	Saprist	Oa3 50–60 cm	264	8.2	2.4	18	75	27.5	ND	ND	ND
Entisol/Histosol	MA	Winooski	Fluvent	Ap 0–25 cm	14.5	1.3	6.9	76	51	1.0	ND	ND	9.0
Entisol/Histosol	MA	Hinckley	Orthent	A 0–3 cm	96.2	3.7	1.5	14	91	5.9			10.0
Acid soil – A	MA	Walpole	Aquept	Apl 0–10 cm	36.9	2.8	1.6	26	52	11.2	3.08	0.12	5.2
Acid soil – A	MA	Paxton1	Udept	Ap 0–13 cm	42.8	2.7	6.2	148	71	2.0	1.6	0.4	15.4
Acid soil – A	MA	Scituate	Udept	Ap 0–20 cm	58.9	4.7	1.6	38	93	2.7	0.9	0.7	3.0
Acid soil – A	MA	Stockbridge	Udept	Ap 0–18 cm	20.2	1.7	6.5	61	87	0.4	1.7	0.3	17.8
Acid soil – A	MA	Scitico	Aquept	Ap 0–18 cm	28.9	2.4	6.3	61	53	2.2	1.5	0.3	16.3
Acid soil – A	MA	Broadbrook	Udept	A 0–3 cm	81.3	4.4	1.4	61	92	4.6	ND	ND	12.9
Acid soil – A	MA	Canton	Udept	A 4–13 cm	31.6	1.2	1.6	27	82	3.6	0.7	0.2	4.4
Acid soil – A	MA	Lanesboro	Udept	E 6–12 cm	29.5	0.8	2.4	38	63	4.6	0.8	0.1	8.3
Acid soil – A	MA	Marlow1	Orthod	A 0–8 cm	60.0	3.7	1.1	21	88	6.7	0.7	0.1	10.7
Acid soil – B	MA	Paxton1	Udept	Bw2 30–43 cm	6.9	0.4	16.4	206	8	0.4	1.81	0.32	16.0
Acid soil – B	MA	Paxton2	Udept	Bw2 23–37 cm	14.4	1.0	8.6	110	48	0.9	0.78	0.76	11.2
Acid soil – B	MA	Paxton2	Udept	Bw4 56–66 cm	3.7	0.3	7.0	132	21	0.4	0.49	0.3	8.3
Acid soil – B	MA	Scituate	Udept	Bw2 30–48 cm	6.5	0.4	6.2	192	48	0.5	0.54	0.35	0.4
Acid soil – B	MA	Stockbridge	Udept	Bw1 18–43 cm	5.5	0.3	10.6	57	32	0.4	1.85	0.27	16.3
Acid soil – B	MA	Scitico	Aquept	Bg1 28–48 cm	4.3	0.3	18.9	100	14	0.2	1.76	0.21	22.2
Acid soil – B	MA	Scitico	Aquept	Bg2 48–74	3.6	0.2	18.0	71	16	0.2	1.5	0.14	29.0
Acid soil – B	MA	Broadbrook	Udept	Bw2 25–38 cm	8.1	0.4	7.1	140	41	0.7	0.99	0.33	3.4
Acid soil – B	MA	Canton	Udept	Bw2 29–42 cm	6.1	0.4	6.6	100	35	0.6	0.48	0.31	5.0
Acid soil – B	MA	Bernardston	Udept	Bw2 11–20 cm	15.0	0.8	14.1	87	34	0.7	1.83	0.65	10.3
Acid soil – B	MA	Bernardston	Udept	Bw3 20–38 cm	7.4	0.5	14.2	93	24	0.4	1.57	0.42	10.5
Acid soil – B	MA	Lanesboro	Udept	Bw1 12–22 cm	30.3	1.2	21.5	126	32	1.0	4.73	0.88	12.5
Acid soil – B	MA	Marlow1	Orthod	Bs2 13–18 cm	46.6	2.5	3.4	55	86	1.9	3.4	0.5	8.0
Acid soil – B	MA	Marlow1	Orthod	Bs3 18–28 cm	31.2	1.7	5.9	148	74	1.4	2.5	0.7	6.9
Acid soil – B	MA	Marlow2	Orthod	Bhs 15–18 cm	72.6	3.5	2.0	30	90	3.7	2.35	0.49	8.1
Alfisol/Mollisol	IN	Brady	Udalf	Ap 0–2 3cm	10.3	0.8	2.4	68	69	1.3	0.7	ND	9.4
Alfisol/Mollisol	NJ	Albia	Udalf	Ap 0–13 cm	13.6	1.8	8.7	97	34	1.0	1	0.2	16.3
Alfisol/Mollisol	NJ	Albia	Udalf	A 0–6 cm	81.1	11.0	3.8	31	75	5.3	ND	ND	18.1
Alfisol/Mollisol	MS	Dundee	Aqualf	Ap 0–8 cm	14.0	1.9	14.0	133	23	0.3	2	0.2	41.3
Alfisol/Mollisol	IN	Odell	Udoll	Ap 0–28 cm	14.5	0.9	8.0	102	72	0.5	ND	ND	25.0
Alfisol/Mollisol	IN	Gumz	Aquoll	Ap 0–23 cm	95.7	7.4	1.3	23	92	6.1	ND	ND	19.2
Ultisol/Oxisol	ML	Howell	Udult	Ap 0–13 cm	46.5	4.0	15.9	84	57	1.2	2.4	0.3	36.3
Ultisol/Oxisol	MD	Glenelg	Udult	Ap 0–13 cm	32.8	3.3	7.8	90	55	1.9	1.5	0.2	19.4
Ultisol/Oxisol	VA	Kibler	Udult	Ap 0–20 cm	64.6	5.8	24.8	111	58	1.1	4.3	1.2	31.0
Ultisol/Oxisol	PR	Unknown	Udox	A 0–10 cm	66.2	3.7	116	99	64	0.6	14.5	0.8	ND

ND: not determined.

## Appendix B. Assumptions used to calculate “paint” and “occlusion” model trajectories in Fig. 2

In both models, we assumed mineral and OM densities of  $2.6 \text{ g cm}^{-3}$  and  $1.4 \text{ g cm}^{-3}$  (Mayer et al., 2004), respectively. The C-constants were calculated from the following formulae based on sorption experiments using model organic compounds and minerals (Mayer, 1999, 2005):  $C\text{-constant} = 100 \exp(-1.61 * \text{fractional coverage})$  where “fractional coverage” is the fraction of total mineral surface covered by OM. The fractional coverage was calculated separately for “paint” and “occlusion” models based on the assumptions below. The data points on each trajectory represent 10% increments from zero to maximal OC concentrations.

The “paint” model (A lines) was calculated with following assumptions: (i) adsorbate is adipic acid with cross-sectional area of  $0.48 \text{ nm}^{-2}$ , (ii) adsorption continues until full monolayer coverage is reached, and (iii) the fraction of mineral surfaces occluded by OM ( $\%SSA_{\text{occlusion}}$ ) is equal to the volumetric ratio of OM to total solids (i.e. mineral plus OM).

The “occlusion” model (B lines) was calculated with following assumptions. (i) SSA of OM is  $1 \text{ m}^2 \text{ g}^{-1}$  (Chiou, 1990; de Jonge and Mittelmeijer-Hazeleger, 1996), (ii) bulk density is  $1.8 \text{ g cm}^{-3}$  and, thus, porosity of 31% at initial point (i.e. no OM), and (iii) OM incrementally fills up pore space (volume not accounted for by mineral solids) until  $\%SSA_{\text{occlusion}}$  reaches 100. The  $\%SSA_{\text{occlusion}}$  in this model was calculated as  $V_{\text{OM}} / (V_{\text{pore space}} - V_{\text{OM}}) * 100$ , where  $V_{\text{OM}}$  is the volume of OM and  $V_{\text{pore space}}$  is the total pore volume in the bulk material which is calculated from the bulk and mineral densities.

## References

- Aiba, S., Kitayama, K., 1999. Structure, composition and species diversity in an altitude-substrate matrix of rain forest tree communities on Mount Kinabalu, Borneo. *Plant Ecol.* 140, 139–157.
- Arnarson, T.S., Keil, R.G., 2001. Organic–mineral interactions in marine sediments studied using density fractionation and X-ray photoelectron spectroscopy. *Org. Geochem.* 32, 1401–1415.
- Benke, M.B., Mermut, A.R., Shariatmadari, H., 1999. Retention of dissolved organic carbon from vinasse by a tropical soil, kaolinite, and Fe-oxides. *Geoderma* 91, 47–63.
- Bock, M.J., Mayer, L.M., 1999. Mesodensity organo-clay associations in a near-shore sediment. *Mar. Geol.* 163, 65–75.
- Brunauer, S., Emmett, P.H., Teller, E., 1938. Adsorption of gases in multimolecular layers. *J. Am. Chem. Soc.* 60, 309–319.
- Chenu, C., Plante, A.F., 2006. Clay-sized organo-mineral complexes in a cultivation chronosequence: revisiting the concept of the ‘primary organo-mineral complex’. *Eur. J. Soil Sci.* 57, 596–607.
- Chiou, C.T., 1990. The surface area of soil organic matter. *Environ. Sci. Technol.* 24, 1164–1166.
- Chorover, J., Amistadi, M.K., 2001. Reaction of forest floor organic matter at goethite, birnessite and smectite surfaces. *Geochim. Cosmochim. Acta* 65, 95–109.
- Chorover, J., Amistadi, M.K., Chadwick, O.A., 2004. Surface charge evolution of mineral-organic complexes during pedogenesis in Hawaiian basalt. *Geochim. Cosmochim. Acta* 68, 4859–4876.
- de Jonge, H., Mittelmeijer-Hazeleger, M.C., 1996. Adsorption of  $\text{CO}_2$  and  $\text{N}_2$  on soil organic matter: nature of porosity, surface area, and diffusion mechanism. *Environ. Sci. Technol.* 30, 408–413.
- de Jonge, H., de Jonge, L.W., Mittelmeijer-Hazeleger, M.C., 2000. The microporous structure of organic and mineral soil materials. *Soil Sci.* 165, 99–108.
- Feller, C., Schouller, E., Thomas, F., Rouiller, J., Herbillon, A.J., 1992.  $\text{N}_2$ -BET specific surface areas of some low activity clay soils and their relationships with secondary constituents and organic matter contents. *Soil Sci.* 153, 293–299.
- Filimonova, S.V., Knicker, H., Kögel-Knabner, I., 2006. Soil micro- and mesopores studied by  $\text{N}_2$  adsorption and  $^{129}\text{Xe}$  NMR of adsorbed xenon. *Geoderma* 130, 218–228.
- Hutchison, C.S., 2005. Geology of North-West Borneo. Sarawak, Brunei and Sabah. Elsevier Science, Amsterdam.
- Jacobson, G., 1970. Gunong Kinabalu Area, Sabah, Malaysia. Geological Survey Malaysia, Kuching, Sarawak.
- Kaiser, K., Guggenberger, G., 2003. Mineral surfaces and soil organic matter. *Eur. J. Soil Sci.* 54, 219–236.
- Kaiser, K., Guggenberger, G., 2007. Sorptive stabilization of organic matter by microporous goethite: sorption into small pores vs. surface complexation. *Eur. J. Soil Sci.* 58, 45–59.
- Keil, R.G., Mayer, L.M., Quay, P.D., Richey, J.E., Hedges, J.I., 1997. Losses of organic matter from riverine particles in deltas. *Geochim. Cosmochim. Acta* 61, 1507–1511.
- Kitayama, K., 1992. Altitudinal transect study of the vegetation on Mount Kinabalu, Borneo. *Vegetatio* 102, 149–171.
- Kitayama, K., Aiba, S., 2002. Ecosystem structure and productivity of tropical rainforests along altitudinal gradients under contrasting soil phosphorus pools on Mount Kinabalu, Borneo. *J. Ecol.* 90, 37–51.
- Kitayama, K., Aiba, S., Takyu, M., Noreen, M.-L., Wagai, R., 2004. Soil phosphorus fractionation and phosphorus-use efficiency of a Bornean tropical montane rain forest during soil ageing with podzolization. *Ecosystems* 7, 259–274.
- Lang, F., Kaupenjohann, M., 2003. Immobilisation of molybdate by iron oxides: effects of organic coatings. *Geoderma* 113, 31–46.
- Mayer, L.M., 1994. Relationships between mineral surfaces and organic carbon concentrations in soils and sediments. *Chem. Geol.* 114, 347–363.
- Mayer, L.M., 1999. Extent of coverage of mineral surfaces by organic matter in marine sediments. *Geochim. Cosmochim. Acta* 63, 207–215.
- Mayer, L.M., 2005. Erratum to L.M. Mayer (1999) “Extent of coverage of mineral surfaces by organic matter in marine sediments” in *Geochimica et Cosmochimica Acta*, 63, 207–215. *Geochim. Cosmochim. Acta* 69, 1375.
- Mayer, L.M., Xing, B., 2001. Organic carbon-surface area-clay relationships in acid soils. *Soil Sci. Soc. Am. J.* 65, 250–258.
- Mayer, L.M., Schick, L.L., Hardy, K., Wagai, R., McCarthy, J., 2004. Organic matter content of small mesopores in sediments and soils. *Geochim. Cosmochim. Acta* 68, 3863–3872.
- McCarthy, J.F., Ilavsky, J., Jastrow, J.D., Mayer, L.M., Perfect, E., Zhuang, J., 2008. Protection of organic carbon in soil microaggregates occurs via restructuring of aggregate porosity and filling of pores with accumulating organic matter. *Geochim. Cosmochim. Acta* 72, 4725–4744.
- Mikutta, C., Lang, F., Kaupenjohann, M., 2004. Soil organic matter clogs mineral pores: evidence from  $^1\text{H-NMR}$  and  $\text{N}_2$  adsorption. *Soil Sci. Soc. Am. J.* 68, 1853–1862.
- Mikutta, R., Kleber, M., Kaiser, K., Jahn, R., 2005. Review: organic matter removal from soils using hydrogen peroxide, sodium hypochlorite, and disodium peroxodisulfate. *Soil Sci. Soc. Am. J.* 69, 120–135.
- Mikutta, R., Kleber, M., Torn, M.S., Jahn, R., 2006. Stabilization of soil organic matter: association with minerals or chemical recalcitrance? *Biogeochemistry* 77, 25–56.
- Mödl, C., Wörmann, H., Amelung, W., 2007. Contrasting effects of different types of organic material on surface area and microaggregation of goethite. *Geoderma* 141, 167–173.
- Murphy, E.M., Zachara, J.M., Smith, S.C., 1990. Influence of mineral-bound humic substances on the sorption of hydrophobic organic compounds. *Environ. Sci. Technol.* 24, 1507–1516.
- Myneni, S.C.B., Brown, J., Martinez, G.A., Meyer-Ilse, W., 1999. Imaging of humic substance macromolecular structures in water and soils. *Science* 286, 1335–1337.
- Pennell, K.D., Boyd, S.A., Abriola, L.M., 1995. Surface area of soil organic matter reexamined. *Soil Sci. Soc. Am. J.* 59, 1012–1018.
- Pichevin, L., Bertrand, P., B. oussafirb, M., Disnarb, J.-R., 2004. Organic matter accumulation and preservation controls in a deep sea modern environment: an example from Namibian slope sediments. *Org. Geochem.* 35, 543–559.
- Pritchard, D.T., Ormerod, E.C., 1976. The effect of heating on the surface area of iron oxide. *Clay Miner.* 11, 327–329.
- Ravikovich, P.I., Bogan, B.W., Neimark, A.V., 2005. Nitrogen and carbon dioxide adsorption by soils. *Environ. Sci. Technol.* 39, 4990–4995.
- Schwertmann, U., 1988. Occurrence and formation of iron oxides in various pedo-environments. In: Stucki, J.W., et al. (Ed.), *Iron in Soils and Clay Minerals*. Reidel, Dordrecht, pp. 267–308.
- Sequi, P., Aringhieri, R., 1977. Destruction of organic matter by hydrogen peroxide in the presence of pyrophosphate and its effect on soil specific surface area. *Soil Sci. Soc. Am. J.* 41, 340–342.
- Soil Survey Staff, 1999. Soil taxonomy: a basic system of soil classification for making and interpreting soil surveys. USDA Natural Resource Conservation Service Agriculture Handbook No. 436, Washington DC, USA.
- Tipping, E., 1981. The adsorption of aquatic humic substances by iron oxides. *Geochim. Cosmochim. Acta* 45, 191–199.
- Vrdoljak, G.A., Sposito, G., 2002. Soil aggregate hierarchy in a Brazilian Oxisol. In: Violante, A., Huang, P.M., Bollag, J.M., Gianfreda, L. (Eds.), *Soil Mineral–Organic Matter–MicroOrganism Interactions and Ecosystem Health, Developments in Soil Science*, 28A. Elsevier Science, Amsterdam, pp. 197–217.
- Wagai, R., Mayer, L.M., 2007. The significance of hydrous iron oxides for organic carbon storage in a range of mineral soils. *Geochim. Cosmochim. Acta* 71, 25–35.
- Wagai, R., Mayer, L.M., Kitayama, K., Knicker, H., 2008. Climate and parent material control on soil organic matter storage, dynamics, and partitioning into physical fractions in undisturbed tropical forest soils. *Geoderma* 147, 23–33.
- Wang, X., Lu, J., Xu, M., Xing, B., 2008. Sorption of pyrene by regular and nanostructured metal oxide particles: influence of adsorbed organic matter. *Environ. Sci. Technol.* 42, 7267–7272.
- Weidler, P.G., Stanjek, H., 1998. The effect of dry heating of synthetic 2-line and 6-line ferrihydrite: II. surface area, porosity and fractal dimension. *Clay Miner.* 33, 277–284.
- Welch, S.A., Vandevivere, P., 1994. Effect of microbial and other naturally occurring polymers on mineral dissolution. *Geomicrobiol. J.* 12, 227–238.
- Welch, S.A., Barkerand, W.W., Banfield, J.F., 1999. Microbial extracellular polysaccharides and plagioclase dissolution — effects of pH,  $\text{CO}_2$ , and organic acids. *Geochim. Cosmochim. Acta* 63, 1405–1419.